Inorg. Chem. **2005**, *44*, 2106–2113

Synthesis and Characterization of Two Quaternary Thorium Chalcophosphates: $Cs_4Th_2P_6S_{18}$ and $Rb_7Th_2P_6Se_{21}$

Benny C. Chan,[†,‡] Ryan F. Hess,[‡] Patrick L. Feng,[†] Kent D. Abney,[‡] and Peter K. Dorhout*[,†]

Department of Chemistry, Colorado State University, Fort Collins, Colorado 80523, and Nuclear Materials and Technology Division (NMT-2), Los Alamos National Laboratory, Los Alamos, New Mexico 87545

Received July 8, 2004

Two new thorium chalcophosphates have been synthesized by the reactive flux method and characterized by single-crystal X-ray diffraction, diffuse reflectance, and Raman spectroscopy: $Cs_4Th_2P_6S_{18}$ (**I**); $Rb_7Th_2P_6Se_{21}$ (**II**). Compound **I** crystallizes as colorless blocks in the triclinic space group $P\bar{1}$ (No. 2) with $a = 12.303(4)$ Å, $b = 12.471(4)$ Å, $c = 12.541(4)$ Å, $\alpha = 114.607(8)°$, $\beta = 102.547(6)°$, $\gamma = 99.889(7)°$, and $Z = 2$. The structure consists of $(Th_2P_6S_{18})^{4-}$ layers separated by layers of cesium cations and only contains the $(P_2S_6)^{4-}$ building block. Compound **II** crystallizes as red blocks in the triclinic pace group $P\bar{1}$ (No. 2) with $a = 11.531(3)$ Å, $b = 12.359(4)$ Å, $c = 16.161(5)$ Å, $\alpha = 87.289(6)°$, $\beta = 75.903(6)°$, $\gamma = 88.041(6)°$, and $Z = 2$. The structure consists of linear chains of $(Th_2P_6Se_{21})^{7-}$ separated by rubidium cations. Compound **II** contains both the $(PSe_4)^{3-}$ and $(P_2Se_6)^{4-}$ building blocks. Both structures may be derived from two known rare earth structures where a rare earth site is replaced by an alkali or actinide metal to form these novel structures. Optical band gap measurements show that compound **I** has a band gap of 2.8 eV and compound **II** has a band gap of 2.0 eV. Solid-state Raman spectroscopy of compound **I** shows the vibrations expected for the $(P_2S_6)^{4-}$ unit. Raman spectroscopy of compound **II** shows the vibrations expected for both $(PSe_4)^{3-}$ and $(P_2Se_6)^{4-}$ units. Our work shows the remarkable diversity of the actinide chalcophosphate system and demonstrates the phase space is still ripe to discover new structures.

Introduction

The molten alkali metal polychalcogenide flux method has produced a myriad of novel and complex compounds.[1] The rare earth chalcophosphate elements made from this method include $K(RE)P_2Se_6$ (RE = Y, La, Ce, Pr, Gd),[2] $K_3CeP_2S_8$,[3] $A_3(RE)P_2Se_8$, and $A_2(RE)P_2Se_7$ (A = Rb, Cs; RE = Ce, Gd).[4] More recently, chalcophosphate compounds were prepared from the actinide elements including β-$K_2ThP_3Se_9$,[5] $Rb_4U_4P_4Se_{26}$,[6] $K_2UP_3Se_9$,[7] $Cs_8U_5(P_3S_{10})_2(PS_4)_4$, $K_{10}Th_3(P_2S_7)_4(PS_4)_2$, $A_5An(PS_4)_3$ (A = K, Rb, Cs; An = U, Th),[8] $K_3Pu(PS_4)_3$, and $APuP_2S_7$ (A = K, Rb, Cs).[9] Our work entails studying the actinide elements and their reactivity in the molten fluxes. We report in this paper two new thorium chalcophosphates, $Cs_4Th_2P_6S_{18}$ and $Rb_7Th_2P_6Se_{21}$, which exist as layered and one-dimensional structures, respectively. Our work shows the remarkable diversity of actinide containing chalcophosphate compounds. The chalcophosphate phase space is still ripe for new actinide-containing structures.

* Author to whom correspondence should be addressed. E-mail: pkd@lamar.colostate.edu. Telephone: (970) 491-0624.

† Colorado State University.

‡ Los Alamos National Laboratory.

(1) Chondroudis, K.; McCarthy, T. J.; Kanatzidis, M. G. *Inorg. Chem.* **1996**, *35*, 840−844. (b) Chung, D. Y.; Iordanidis, L.; Choi, K. S.; Kanatzidis, M. G. *Bull. Kor. Chem. Soc.* **1998**, *19*, 1283−1293. (c) Kanazidis, M. G.; Sutorik, A. C. *Prog. Inorg. Chem.* **1995**, *43*, 151−265. (d) Sutorik, A. C.; Kanatzidis, M. G. *Chem. Mater.* **1997**, *9*, 387−398. (e) Narducci, A. A.; Ibers, J. A. *Chem. Mater.* **1998**, *10*, 2811−2823.

(2) Chen, J. H.; Dorhout, P. K.; Ostenson, J. E. *Inorg. Chem.* **1996**, *35*, 5627−5633.

(3) Gauthier, G.; Jobic, S.; Brec, R.; Rouxel, J. *Inorg. Chem.* **1998**, *37*, 2332−2333.

(4) Chondroudis, K.; Kanatzidis, M. G. *Inorg. Chem.* **1998**, *37*, 3793−3797.

(5) Briggs-Piccoli, P. M.; Abney, K. D.; Dorhout, P. K. *J. Nucl. Sci. Technol.* **2002**, *Suppl. 3*, 611−615.

(6) Chondroudis, K.; Kanazidis, M. G. *J. Am. Chem. Soc.* **1997**, *119*, 2574−2575.

(7) Chondroudis, K.; Kanatzidis, M. G. *C. R. Acad. Sci. Paris* **1996**, *t. 322, Ser. Iib*, 887.

(8) Hess, R. F.; Abney, K. D.; Burris, J. L.; Hochheimer, H. D.; Dorhout, P. K. *Inorg. Chem.* **2001**, *40*, 2851−2859.

(9) Hess, R. F.; Gordon, P. L.; Tait, C. D.; Abney, K. D.; Dorhout, P. K. *J. Am. Chem. Soc.* **2002**, *124*, 1327−1333.

10.1021/ic049101e CCC: $30.25 © 2005 American Chemical Society
Published on Web 02/22/2005

Table 1. Select Crystallographic Data for $Cs_4Th_2P_6S_{18}$ and $Rb_7Th_2P_6Se_{21}$

	$Cs_4Th_2P_6S_{18}$ (**I**)	$Rb_7Th_2P_6Se_{21}$ (**II**)
fw	879.31	2906.35
a, Å	12.303(4)	11.531(3)
b, Å	12.471(4)	12.359(4)
c, Å	12.541(4)	16.161(5)
α, deg	114.607(8)	87.289(6)
β, deg	102.547(6)	75.903(6)
γ, deg	99.889(7)	88.041(6)
V, Å^3	1631.5(9)	2230.7(11)
Z	2	2
λ(Mo Kα), Å	0.710 73	0.710 73
space group	$P\bar{1}$ (No. 2)	$P\bar{1}$ (No. 2)
temp, K	163	298
ρ_{calcd}, g/cm^3	3.580	4.327
μ, mm^{-1}	14.951	31.602
R1,[a] %	0.0421	0.0433
wR2,[b] %	0.0916	0.0979

[a] $R1 = \Sigma||F_o| - |F_c||/\Sigma|F_o|$. [b] $wR2 = [\Sigma[w(F_o^2 - F_c^2)^2]/\Sigma[w(F_o^2)^2]]^{1/2}$.

Table 2. Fractional Atomic Coordinates and Equivalent Isotropic Displacement Parameters (10^3Å^2)[a] for $Cs_4Th_2P_6S_{18}$

	x	y	z	*U*(eq)
Th(1)	0.6466(1)	0.6783(1)	−0.0041(1)	8(1)
Th(2)	1.3900(1)	0.7148(1)	−0.3203(1)	8(1)
Cs(1)	0.9004(1)	0.4317(1)	−0.2606(1)	15(1)
Cs(2)	1.1242(1)	0.8535(1)	−0.1024(1)	17(1)
Cs(3)	1.1692(1)	0.2283(1)	−0.4459(1)	22(1)
Cs(4)	1.6495(1)	1.0745(1)	−0.2719(1)	21(1)
P(1)	0.7844(3)	0.4532(3)	0.0119(3)	10(1)
P(2)	1.3167(3)	0.5831(3)	−0.1261(3)	10(1)
P(3)	1.2352(3)	1.2007(3)	0.1883(3)	10(1)
P(4)	1.3552(3)	0.3649(3)	−0.6412(3)	8(1)
P(5)	1.3007(3)	1.0301(3)	−0.2537(3)	10(1)
P(6)	0.7749(3)	0.1302(3)	−0.5556(3)	10(1)
S(1)	0.6630(3)	0.4282(3)	−0.1398(3)	11(1)
S(2)	0.8442(3)	0.7261(3)	−0.876(3)	12(1)
S(3)	0.5999(3)	0.8180(3)	0.2452(3)	14(1)
S(4)	0.8544(3)	0.6391(3)	0.1254(3)	11(1)
S(5)	0.5357(2)	0.5587(3)	−0.2886(3)	10(1)
S(6)	0.4261(3)	0.7567(3)	−0.0510(3)	11(1)
S(7)	0.6438(3)	0.8651(3)	−0.1110(3)	11(1)
S(8)	0.8261(3)	0.9182(3)	0.1854(3)	13(1)
S(9)	0.5816(3)	0.5312(3)	0.1366(3)	11(1)
S(10)	1.1532(3)	0.7317(3)	−0.4099(3)	12(1)
S(11)	1.2639(3)	0.4695(3)	−0.5540(3)	12(1)
S(12)	1.3989(3)	0.9598(3)	−0.1593(3)	14(1)
S(13)	1.2052(3)	0.5530(3)	−0.2873(3)	12(1)
S(14)	1.5553(3)	0.7108(3)	−0.4492(3)	12(1)
S(15)	1.3698(3)	0.8295(3)	−0.4835(3)	14(1)
S(16)	0.8780(3)	0.0980(3)	−0.4360(3)	16(1)
S(17)	1.1342(3)	1.0857(3)	0.2221(3)	16(1)
S(18)	1.1117(3)	0.6518(3)	0.0210(3)	13(1)

[a] *U*(eq) is defined as one-third the trace of the orthogonalized $\mathbf{U}_{ij}$ tensor.

Experimental Section

General Synthesis. Red phosphorus powder (99.9%) was purchased from Cerac. Selenium shot (99.999%) was purchased from Johnson Matthey. ^{232}Th ribbon was obtained from Los Alamos National Laboratory. Alkali metal chalcogenide salts, A_2Q_5 (A = Rb, Cs, Q = S, Se), were prepared from a stoichiometric ratio of elements in liquid ammonia as described elsewhere.[10] *N*,*N*-dimethylformamide (DMF) was purchased from Aldrich and used without further purification. Ampules for the reactions were fused-silica with 10 mm inner diameter and a 12 mm outer diameter.

(10) Liao, J.-H.; Kanatzidis, M. G. *Inorg. Chem.* **1992**, *31*, 431−439.

Table 3. Bond Distances (Å) for $Cs_4Th_2P_6S_{18}$

Th(1)−S(2)	2.914(3)	P(1)−S(1)	2.016(4)
Th(1)−S(1)	2.934(3)	P(1)−S(4)	2.044(4)
Th(1)−S(4)	2.949(3)	P(2)−S(13)	2.024(4)
Th(1)−S(8)	3.001(3)	P(2)−S(6)	2.034(4)
Th(1)−S(9)	3.051(3)	P(2)−S(9)	2.035(4)
Th(1)−S(6)	3.059(3)	P(3)−S(17)	1.975(4)
Th(1)−S(5)	3.094(3)	P(3)−S(2)	2.029(4)
Th(1)−S(3)	3.119(3)	P(3)−S(7)	2.053(4)
Th(1)−S(7)	3.136(3)	P(4)−S(11)	2.002(4)
Th(1)−S(9A)	3.150(3)	P(4)−S(14)	2.024(4)
Th(2)−S(12)	2.842(3)	P(4)−S(5)	2.063(4)
Th(2)−S(14)	2.854(3)	P(5)−S(8)	2.012(4)
Th(2)−S(15)	2.939(3)	P(5)−S(3)	2.019(4)
Th(2)−S(5A)	2.949(3)	P(6)−S(16)	1.967(4)
Th(2)−S(10)	2.964(3)	P(6)−S(15)	2.035(4)
Th(2)−S(13)	2.991(3)	P(6)−S(10)	2.049(4)
Th(2)−S(11)	3.047(3)	P(1)−P(2)	2.219(4)
Th(2)−S(6A)	3.110(3)	P(3)−P(4)	2.211(4)
Th(2)−S(7A)	3.238(3)	P(5)−P(6)	2.235(4)
P(1)−S(18)	1.967(4)		

Warning: *^{232}Th is a radioactive element with a half-life of 1.41 × 10^{10} years. Although its radioactivity is low, the daughter products of decay can render the samples highly radioactive over time.*

Synthesis of $Cs_4Th_2P_6S_{18}$ (I). $Cs_4Th_2P_6S_{18}$ or $Cs_4Th_2(P_2S_6)_3$ was prepared from a mixture of 0.0590 g (0.254 mmol) of Th, 0.0473 g (1.52 mmol) of P, 0.5771 g (1.77 mmol) of S, and 0.217 g (0.500 mmol) of Cs_2S_5. The mixture was loaded into a fused-silica ampule in a nitrogen glovebox and sealed under vacuum. The ampule was heated to 500 °C at a rate of 30 °C/h and held there for 288 h. The ampule was cooled to room temperature at a rate of 3 °C/h. The ampule was opened in a nitrogen glovebox, and the excess flux was washed with DMF. The colorless blocks isolated were air and moisture sensitive. A single crystal was selected for analysis by X-ray diffraction at 163 K. A collection of the colorless blocks were hand picked for Raman and diffuse reflectance measurements. The sample appeared to be stable during the collection of Raman and diffuse reflectance spectra.

Synthesis of $Rb_7Th_2P_6Se_{21}$ (II). $Rb_7Th_2P_6Se_{21}$ or $Rb_7Th_2(PSe_4)_3(P_2Se_6)_{1.5}$ was prepared from a mixture of 0.0901 g (0.388 mmol) of Th, 0.0383 g (1.24 mmol) of P, 0.0980 g (1.24 mmol) of Se, and 0.3830 g (0.677 mmol) of Rb_2Se_5. The mixture was loaded into a fused-silica ampule in a nitrogen glovebox and sealed under vacuum. The ampule was heated to 500 °C at a rate of 30 °C/h and held there for 288 h. The ampule was cooled to room temperature at a rate of 3 °C/h. The ampule was opened in air, and the excess flux was washed with DMF. A single crystal was selected

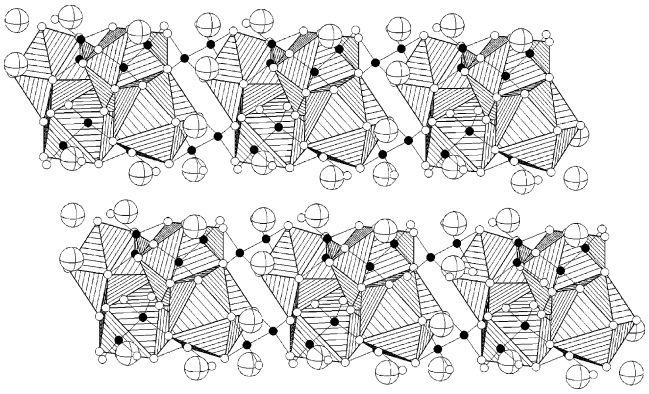

Figure 1. Polyhedral view of the layered $Cs_4Th_2P_6S_{18}$. Equatorial circles are Cs, open circles are S, filled circles are P, and striped polyhedra are Th.

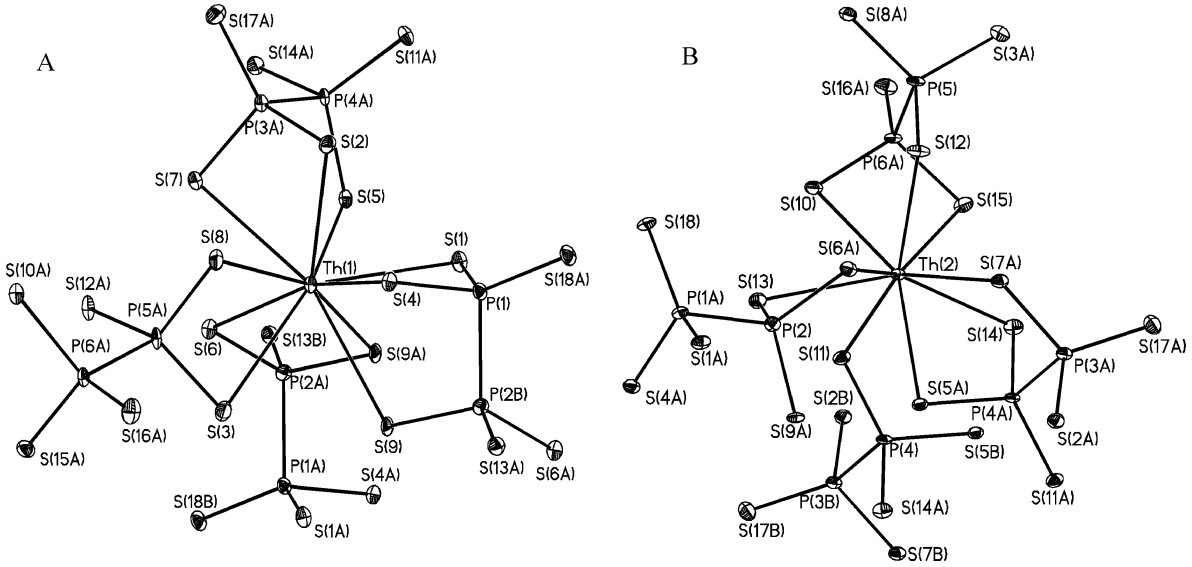

Figure 2. Thermal ellipsoid plots at 50% showing (a) the 10-coordinate binding environment of Th(1) and (b) the 9-coordinate binding environment of Th(2) in $Cs_4Th_2P_6S_{18}$.

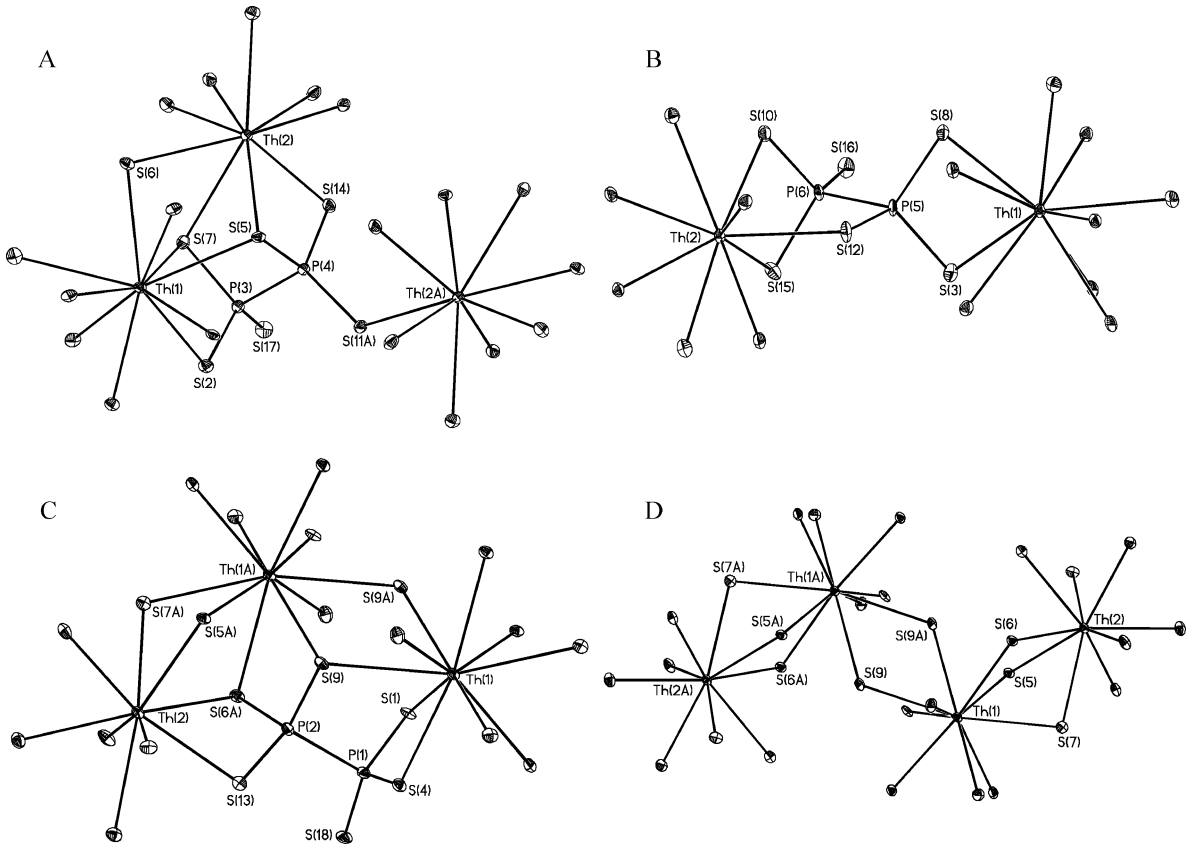

Figure 3. Thermal ellipsoid plots at 50% showing (a−c) the three binding modes of $(P_2S_6)^{4-}$ and (d) the tetramer of thorium in $Cs_4Th_2P_6S_{18}$.

for analysis by X-ray diffraction. A collection of the red blocks were hand picked for Raman and diffuse reflectance measurements. The red blocks decomposed when ground into a fine powder. A stoichiometric mixture of the elements did not produce red crystals of $Rb_7Th_2P_6Se_{21}$.

Physical Measurements. Single-Crystal X-ray Diffraction. Intensity data sets were collected using a Bruker Smart CCD diffractometer. These data were integrated using SAINT,[11] a SADABS correction was applied,[12] and the structures were solved by direct methods using SHELXTL.[13] Crystallographic data for compound **I** and **II** are reported in Table 1.

Raman Spectroscopy. The bulk solid-state Raman spectrum of compound **I** was recorded on a home-built optical bench using an Acton Research Spectra Pro-275 liquid-N_2-cooled CCD detector (256 × 1024) using a controller model ST130 and a 50 mW HeNe

(11) *SAINT; Data processing software for the SMART system*; Bruker Analytical X-ray Instruments, Inc.: Madison, WI, 1995.

(12) Sheldrick, G. M. *SADABS*; University of Gottingen: Gottingen, Germany, 1997.

(13) *SHELXTL 6.1*; Bruker AXS Inc.: Madison, WI, 2000.

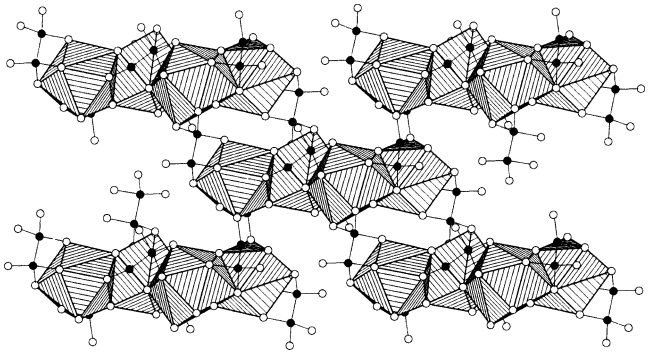

Figure 4. Polyhedral view of the $[Th_2P_6S_{18}]^{4-}$ layer in $Cs_4Th_2P_6S_{18}$. Cs atoms were removed for clarity, open circles are S, filled circles are P, and striped polyhedra are Th.

laser line at 632.8 nm. The bulk solid-state Raman spectrum of compound **II** was recorded on a Nicolet Magna-IR 760 spectrometer with a FT-Raman module attachment by use of a Nd:YAG excitation laser (1064 nm).

UV−Visible Spectroscopy. Diffuse reflectance measurements were recorded on a Varian Cary 500 Scan UV−vis−NIR spectrophotometer equipped with a Praying Mantis accessory. A Teflon standard was used as a reference. The Kubelka−Munk function was applied to obtain band-gap information.[14]

Results and Discussion

$Cs_4Th_2P_6S_{18}$ (I). A single clear crystal of $Cs_4Th_2P_6S_{18}$ was selected, 10 977 (7605 independent) reflections were collected, and an absorption correction was applied (R_{int} = 0.0363). Data were collected within a θ range of 1.77−28.27° to a completeness of 93.7% with a data index range of $-14 \le h \le 16$, $-16 \le k \le 9$, and $-16 \le l \le 16$. The structure was solved in $P\bar{1}$ by direct methods with final electron density residuals of 5.200 and −3.500 e Å^{-3}. The residual electron density was slightly higher than expected and was attributed to an absorption correction problem with thorium. All atoms were refined anisotropically on F^2 for 272 variables.[13] Select crystallographic data, atom positions, and a list of selected bond distances are listed in Tables 1−3.

The compound is composed of two-dimensional $[Th_2P_6S_{18}]^{4-}$ layers, Figure 1. The cesium ions reside between the layers and inside holes within each layer. Two crystallographically independent thorium atoms exist in the structure. Th(1) is coordinated to 10 sulfur atoms in a sphenocoronal geometry, Figure 2a. Th(2) is coordinated to nine sulfur atoms in a distorted tricapped trigonal prism, Figure 2b. The Th(1)−S bond distances range from 2.914(3) to 3.150(3) Å with an average distance of 3.04(8) Å. The Th(2)−S bond distances range from 2.842(3) to 3.238(3) Å with an average distance of 2.99(1) Å. These bond distances are expected for Th^{4+}. The thorium polyhedra are linked by three distinct ethane-like $(P_2S_6)^{4-}$ building blocks to form the layers. The 5-fold coordinate binding of $(P_2S_6)^{4-}$ modes are shown in Figure 3a−c. The $(P_2S_6)^{4-}$ building block contains a P−P bond making the phosphorus formally tetravalent. Each building block coordinates five of its six sulfur atoms to one or more atoms. The sixth sulfur atom is terminal and bonded to phosphorus and cesium cations. No terminal sulfur atoms are bonded to Th(1) or Th(2); all sulfur atoms belong to thiophosphate building blocks.

The fundamental unit in each $[Th_2P_6S_{18}]^{4-}$ layer is a tetramer of thorium polyhedra. Each tetramer is linked to neighboring tetramers through two $(P_2S_6)^{4-}$ building blocks. Figure 4 illustrates a single $[Th_2P_6S_{18}]^{4-}$ layer, while Figure

(14) Wilkinson, F.; Kelly, G. *CRC Handbook of Organic Photochemistry*; Scaiano, J. C., Ed.; CRC Press: Boca Raton, FL, 1989; Vol. 1, pp 293−314.

Table 4. Fractional Atomic Coordinates and Equivalent Isotropic Displacement Parameters (10^3Å^2)[a] for $Rb_7Th_2P_6Se_{21}$

	x	y	z	*U*(eq)
Th(1)	0.7954(1)	0.6438(1)	0.5125(1)	22(1)
Th(2)	0.8584(1)	0.6834(1)	0.8493(1)	21(1)
Rb(1)	0.7278(2)	0.4930(2)	1.2500(1)	35(1)
Rb(2)	0.9572(2)	0.9915(2)	0.6493(1)	49(1)
Rb(3)	0.4730(2)	1.0031(2)	0.8266(1)	46(1)
Rb(4)	0.4063(2)	0.8330(2)	0.5922(1)	49(1)
Rb(5)	0.3686(2)	0.7030(2)	1.0147(1)	50(1)
Rb(6)	0.7208(2)	1.3112(2)	0.6834(1)	54(1)
Rb(7)	0.9326(2)	0.8306(2)	1.1049(1)	46(1)
P(1)	0.9170(4)	0.4641(4)	0.9934(3)	24(1)
P(2)	0.7781(4)	0.9764(4)	0.9163(3)	21(1)
P(3)	0.9238(4)	0.3570(4)	0.4063(3)	21(1)
P(4)	0.5925(4)	0.6582(4)	0.7495(3)	21(1)
P(5)	0.5754(4)	0.7799(4)	1.3476(3)	20(1)
P(6)	1.2535(4)	1.1478(4)	0.6424(3)	22(1)
Se(1)	1.0182(2)	0.7637(2)	0.5058(1)	28(1)
Se(2)	0.6376(2)	0.5605(2)	0.8562(1)	35(1)
Se(3)	0.7772(2)	0.5897(2)	1.0301(1)	32(1)
Se(4)	0.8802(2)	0.7169(2)	0.3274(1)	26(1)
Se(5)	0.7548(2)	0.7573(2)	0.6945(1)	32(1)
Se(6)	0.5649(2)	0.6455(1)	0.4448(1)	27(1)
Se(7)	0.9448(2)	0.4437(2)	0.8557(1)	27(1)
Se(8)	0.7285(2)	0.8792(2)	0.4942(1)	28(1)
Se(9)	0.6600(2)	0.8339(2)	0.9354(1)	29(1)
Se(10)	1.0955(2)	0.6830(2)	0.9271(1)	32(1)
Se(11)	0.4239(2)	0.7405(2)	0.7928(1)	37(1)
Se(12)	0.9538(2)	0.8979(2)	0.8597(1)	32(1)
Se(13)	0.5841(2)	0.5546(2)	0.6442(1)	30(1)
Se(14)	0.7441(2)	0.4177(2)	0.4638(1)	31(1)
Se(15)	0.7430(2)	1.0983(2)	0.8226(1)	43(1)
Se(16)	0.5985(2)	0.7321(2)	1.2182(1)	34(1)
Se(17)	1.0851(2)	0.7214(2)	0.7102(1)	34(1)
Se(18)	1.2149(2)	1.0083(2)	0.7257(1)	36(1)
Se(19)	0.4358(2)	0.9024(2)	1.3860(1)	32(1)
Se(20)	0.9526(2)	0.5071(2)	0.6144(2)	75(1)
Se(21)	0.7857(2)	1.0528(2)	1.0308(1)	41(1)

[a] *U*(eq) is defined as one-third the trace of the orthogonalized $\mathbf{U}_{ij}$ tensor.

Table 5. Bond Distances for $Rb_7Th_2P_6Se_{21}$

Th(1)−Se(1)	2.986(2)	P(2)−Se(21)	2.137(5)
Th(1)−Se(8)	3.004(2)	P(2)−Se(15)	2.184(5)
Th(1)−Se(4)	3.0167(19)	P(2)−Se(12)	2.221(5)
Th(1)−Se(13)	3.020(2)	P(2)−Se(9)	2.228(5)
Th(1)−Se(14)	3.054(2)	P(3)−Se(17)	2.182(5)
Th(1)−Se(6)	3.111(2)	P(3)−Se(20)	2.201(5)
Th(1)−Se(20)	3.136(2)	P(3)−Se(1)	2.210(5)
Th(1)−Se(5)	3.243(2)	P(3)−Se(14)	2.178(5)
Th(2)−Se(12)	2.933(2)	P(4)−Se(5)	2.244(5)
Th(2)−Se(2)	2.985(2)	P(4)−Se(2)	2.213(5)
Th(2)−Se(9)	3.0058(19)	P(4)−Se(11)	2.138(5)
Th(2)−Se(3)	3.030(2)	P(4)−Se(13)	2.200(5)
Th(2)−Se(17)	3.038(2)	P(5)−Se(6)	2.216(5)
Th(2)−Se(7)	3.097(2)	P(5)−Se(19)	2.169(5)
Th(2)−Se(5)	3.111(2)	P(5)−Se(16)	2.152(4)
Th(2)−Se(10)	3.275(2)	P(5)−P(6)	2.237(7)
P(1)−Se(10)	2.163(5	P(6)−Se(8)	2.208(5)
P(1)−Se(7)	2.197(4)	P(6)−Se(4)	2.224(5)
P(1)−Se(3)	2.193(5)	P(6)−Se(18)	2.126(5)
P(1)−P(1)	2.197(10)		

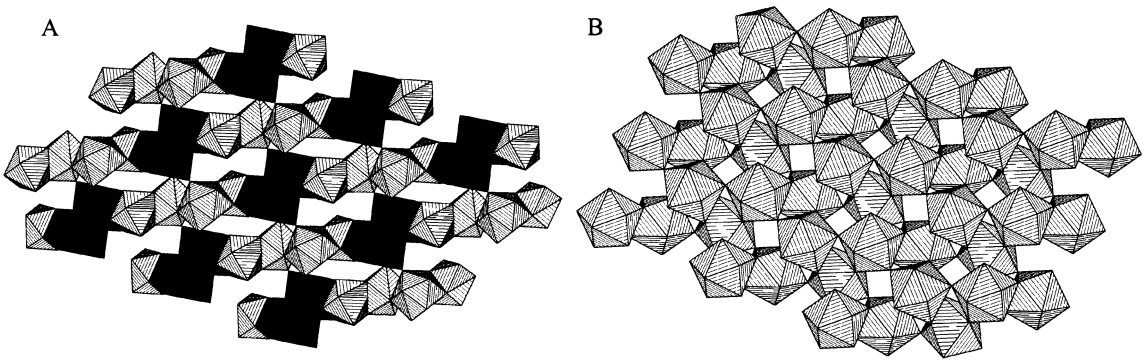

Figure 5. (a) Polyhedral view of $Cs_4Th_2P_6S_{18}$ with thorium as striped polyhedra and Cs(4) as black polyhedra showing a completed layer that is similar to (b) the $[LaP_2S_6]^-$ layers in $KLaP_2S_6$. Phosphorus and other alkali metals were removed for clarity.

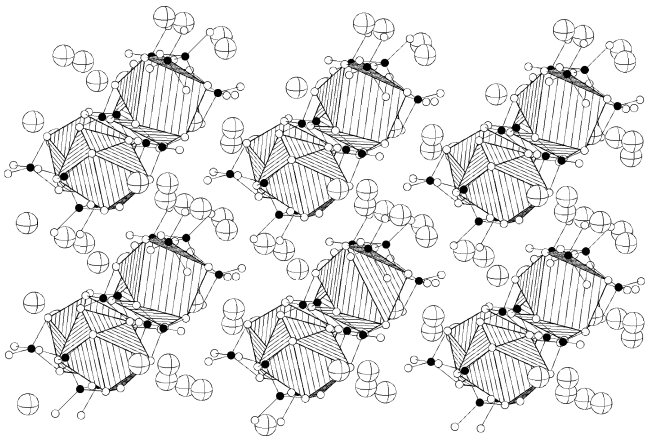

Figure 6. Polyhedral view down the *c*-axis of $Rb_7Th_2P_6Se_{21}$. Equatorial circles are Rb, open circles are Se, filled circles are P, and polyhedra are Th.

3d illustrates the coordination within a single tetramer unit. Each tetramer contains two Th(1) and two Th(2) polyhedra; the two Th(1) polyhedra form the interior portion of the unit and are edged shared through S(9) and S(9A) while the two Th(2) polyhedra cap the unit by sharing the triangular face containing S(5), S(6), and S(7).

Compound **I** has no known rare earth analogues; however, the layered structure is related to the class of rare earth compounds with the empirical formula $AREP_2Q_6$ (A = Na, K; RE = La, Ce, Pr, Sm, Gd; Q = S, Se)[15] by the following consideration:

$$ALaP_2Q_6 \times 3 = A_3La_3P_6Q_{18}$$

$$3(La^{III}) \equiv 2(Th^{IV}) + A^{I}$$

$$A_3La_3P_6Q_{18} \equiv A_4Th_2P_6Q_{18}$$

Both **I** and $AREP_2Q_6$ are layered structures with the ethane-like $(P_2Q_6)^{4-}$ building block. The coordination environments around Th(2) and the rare earth are similar, coordinating nine chalcogenides belonging to four building blocks. Two $(P_2Q_6)^{4-}$ building blocks are coordinated to the metal in a face-shared arrangement, one building block is edge-shared, and one is corner shared. Compound **I** does

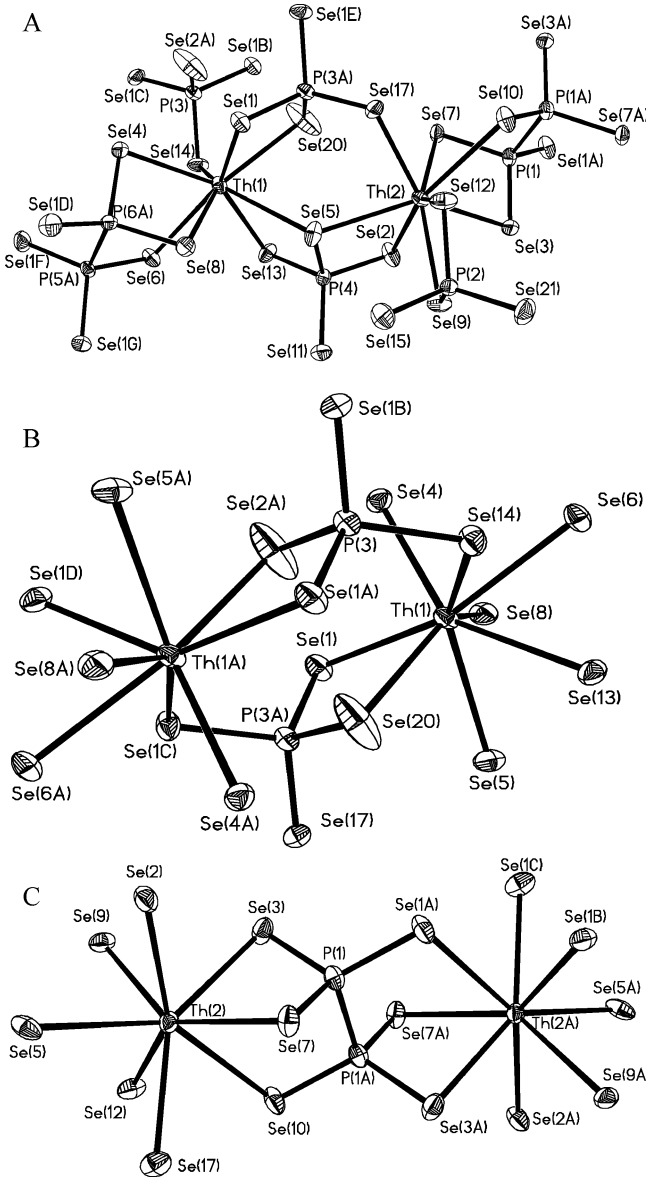

Figure 7. Thermal ellipsoid plots at 50% of $Rb_7Th_2P_6Se_{21}$ showing (a) the 8-coordinate binding environment of Th(1) and Th(2) linked by two $(PSe_4)^{3-}$ building blocks, (b) the binding environment between adjacent Th(1) with two tridentate $(PSe_4)^{3-}$ building blocks, and (c) the binding environment between adjacent Th(2) with a hexadentate $(P_2Se_6)^{4-}$ building block.

(15) Chen, J. H.; Dorhout, P. K. *Inorg. Chem.* **1995**, *34*, 5705−5706. (b) Evanson, C. R.; Dorhout, P. K. *Inorg. Chem.* **2001**, *40*, 2884−2891. (c) Chen, J. H.; Dorhout, P. K. *Inorg. Chem.* **1996**, *35*, 5627−5633. (d) Aitken, J. A.; Evain, M.; Iordanidis, L.; Kanatzidis, M. G. *Inorg. Chem.* **2002**, *41*, 180−191. (e) Goh, E.-Y.; Kim, E.-J.; Kum, S.-J. *J. Solid State Chem.* **2001**, *160*, 195−204.

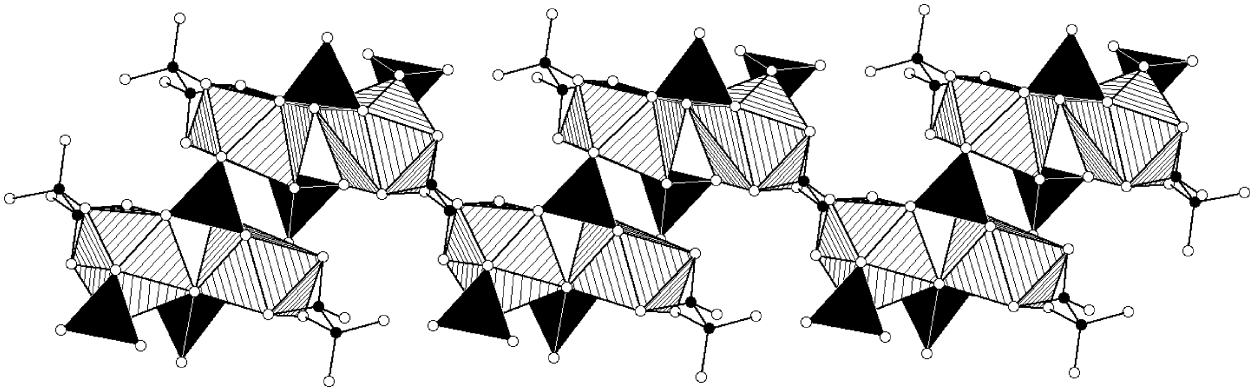

Figure 8. Polyhedral view of the $[Th_2P_6Se_{21}]^{7-}$ 1-dimensional chain in $Rb_7Th_2P_6Se_{21}$. Rb atoms were removed for clarity. Open circles are Se, black circles are P, black polyhedra are the $(PSe_4)^{3-}$ building blocks, and striped polyhedra are Th.

not have a herringbone structure of the P−P bonds when viewed along the *z* direction as seen in $AREP_2Q_6$. If the Cs(4) atoms in $Cs_4Th_2P_6S_{18}$ were drawn as polyhedra, Figure 5a, compound **I** would have a complete layer of interconnected polyhedra similar to $AREP_2Q_6$, Figure 5b. Since thorium exists as a tetravalent species, the compound will not charge balance if the $AREP_2Q_6$ structure is adopted. A cesium atom occupies a site in the layer to form the new structure of compound **I**. The compound requires the alkali metal for a stable structure as the reaction did not form a thorium analogue of UP_2S_6 which is also charge balanced but has an unrelated structure.[16]

$Rb_7Th_2P_6Se_{21}$ (II). A single red crystal of $Rb_7Th_2P_6Se_{21}$ was selected, 17 968 (9629 independent) reflections were collected, and an absorption correction was applied (R_{int} = 0.1124). Data were collected within a θ range of 1.30−28.31° to a completeness of 86.7% with a data index range of $-15 \le h \le 15$, $-16 \le k \le 16$, and $-21 \le l \le 21$. The structure was solved in $P\bar{1}$ by Patterson methods with final electron density residuals of 2.521 and −2.147 e Å^{-3}. All atoms were refined anisotropically on F^2 for 325 variables.[13] Select crystallographic data, atom positions, and a list of selected bond distances are listed in Tables 1, 4, and 5.

Compound **II** is composed of one-dimensional $[Th_2P_6Se_{21}]^{7-}$ chains running along the *c*-direction, Figure 6. The rubidium cations surround the chains and provide charge balance in the structure. Two crystallographically unique thoriums exist in this structure. The thorium environment is shown in Figure 7a. Both are coordinated by 8 selenium atoms in a distorted bicapped trigonal prism geometry. The Th(1)−Se bond distances range from 2.986(2) to 3.243(2) Å with an average of 3.071(2) Å. The Th(2)−Se bond distances range from 2.932(2) to 3.275(2) Å with an average of 3.059(2) Å. The bond distances are expected for Th^{4+}. The thorium polyhedra are also interconnected by two selenophosphate building blocks, the ethane-like $[P_2Se_6]^{4-}$, and the tetrahedral $[PSe_4]^{3-}$. The $[P_2Se_6]^{4-}$ unit contains a P−P bond making the oxidation state of the phosphorus formally tetravalent. The phosphorus in $[PSe_4]^{3-}$ is formally pentavalent. The compound is charged balanced with thorium being formally tetravalent.

The one-dimensional chains are seen in Figure 8. Th(1) and Th(2) polyhedra are corner-shared through Se(5) and 3-fold coordination of a $[PSe_4]^{3-}$ tetrahedron, Figure 8. Th(1) atoms are connected together through two tetrahedral $[PSe_4]^{3-}$ units, Figure 7b, creating a tetramer of thorium polyhedra. The tetramers are connected to each other through ethane-like $[P_2Se_6]^{4-}$ units and Th(2) polyhedra, Figure 7c, creating a zigzag one-dimensional ribbon. All selenium atoms coordinated by thorium are part of a selenophosphate building block. Th(2) is capped by a 2-fold coordinate $[PSe_4]^{3-}$ unit while Th(1) is capped by a 3-fold coordinate $[P_2Se_6]^{4-}$ unit.

The mixed tetrahedral and ethane-like building blocks are found in the class of compounds with the formula $A_2REP_2Q_7$ (A = K, Rb, Cs; RE = La, Ce, Sm; Q = S, Se).[15b,15e,17] The $Rb_7Th_2P_6Se_{21}$ structure has no known rare earth analogues yet is related by the following consideration:

$$A_2LaP_2Q_7 \times 3 = A_6La_3P_6Q_{21}$$

$$3(La^{III}) \equiv 2(Th^{IV}) + A^{I}$$

$$A_6La_3P_6Q_{21} \equiv A_7Th_2P_6Q_{21}$$

The metal polyhedra of $A_2REP_2Q_7$ form one-dimensional chains that are interconnected by $(PQ_4)^{3-}$ tetrahedra similar to **II**. The chains then form a two-dimensional layer using $(P_2Q_6)^{4-}$ units through the same 6-fold coorination as seen in **II**, Figure 10. If the site occupied by the Rb(3) atom in **II** is drawn as a polyhedron, Figure 9a, the one-dimensional chains would connect and the compound would have the same two-dimensional layer as $A_2REP_2Q_7$, Figure 9b. Once again, due to the charge balance issues discussed for compound **I**, the structure adopts the novel one-dimensional actinide chain structure by substitution of an alkali metal in the layer. Moreover, one expects that as the ratio of alkali metal to actinide metal increases, the dimensionality of the structure changes from a two-dimensional structure to a one-dimensional structure.

Several examples of one-dimensional chalcophosphate compounds[18] and one-dimensional compounds with mixed

(16) Do, J.; Kim, J.; Lah, S.; Yun, H. *Bull. Korean Chem. Soc.* **1993**, *14*, 678.

(17) Evanson, C. R.; Dorhout, P. K. *Inorg. Chem.* **2001**, *40*, 2875−2883. (b) Chondroudis, K.; Kanatzidis, M. G. *Inorg. Chem.* **1998**, *37*, 3792−3797.

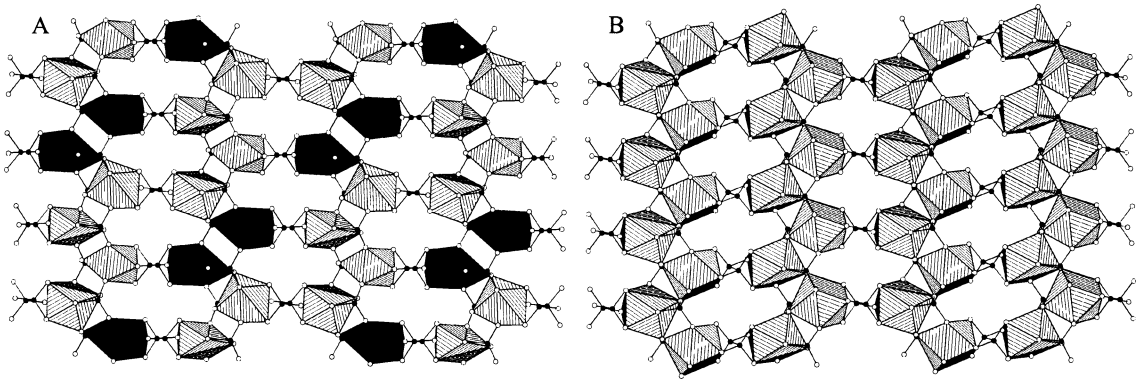

Figure 9. (a) Polyhedral view of $Rb_7Th_2P_6Se_{21}$ with thorium as striped polyhedra and Rb(3) as black polyhedra showing a two-dimensional layer that is similar to (b) the $[LaP_2S_7]^-$ layers found in $KLaP_2S_7$. Phosphorus atoms are shown as closed circles, selenium and sulfur are shown as open circles, and other alkali atoms were removed for clarity.

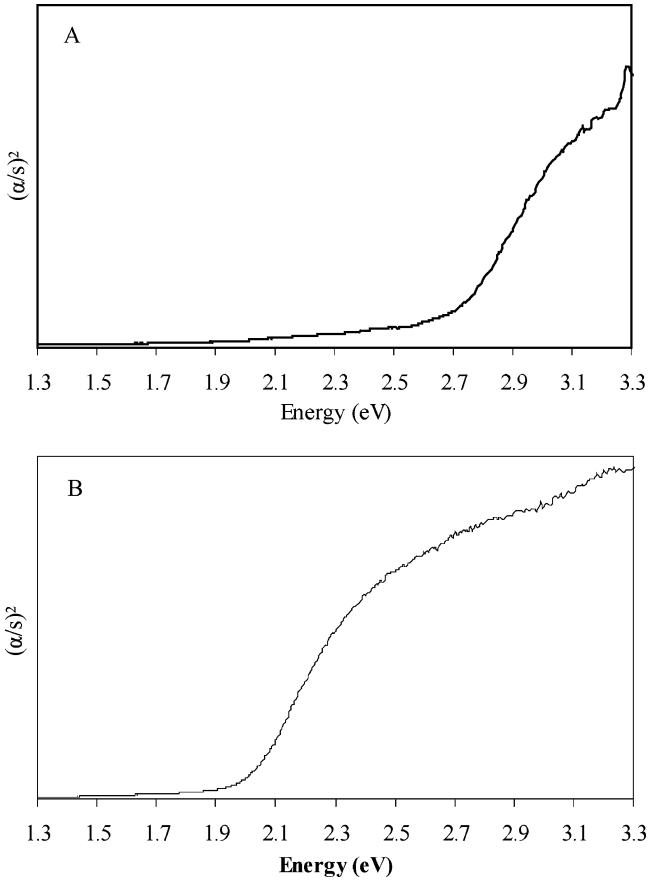

Figure 10. Diffuse reflectance spectra in Kubelka−Munk units of (a) $Cs_4Th_2P_6S_{18}$ and (b) $Rb_7Th_2P_6Se_{21}$.

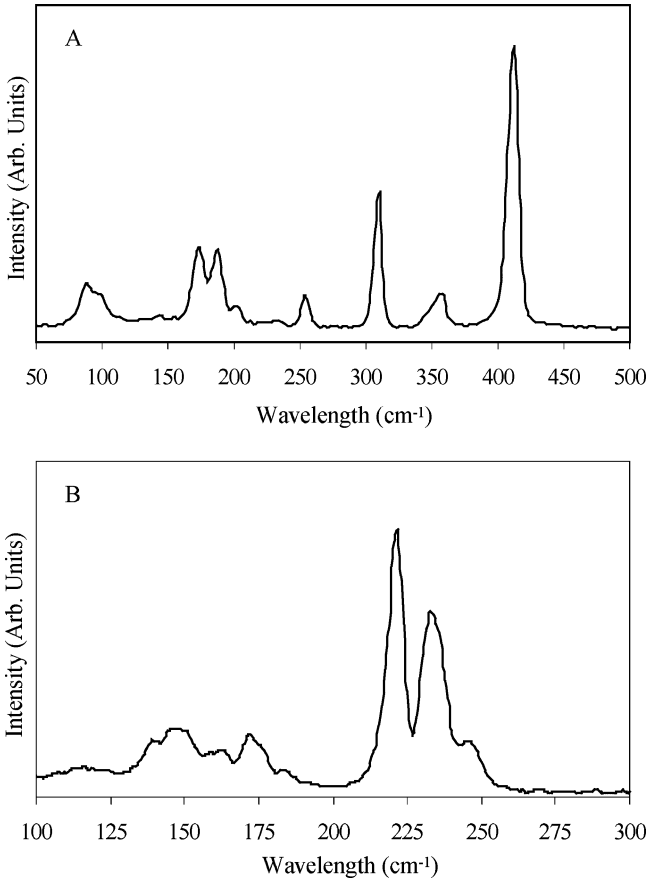

Figure 11. Raman spectra of (a) $Cs_4Th_2P_6S_{18}$ and (b) $Rb_7Th_2P_6Se_{21}$.

building blocks[19] are reported in the literature. $K_4In_2(PSe_5)_2(P_2Se_6)$[20] and $K_2MP_2S_7$ (M = Cr, V)[21] most closely resemble the chains seen in **II**. The compounds form edge-shared dimers that are interconnected by two $(PSe_5)^{3-}$ or $(PSe_4)^{4-}$ units. The dimers are then linked together by a tetradentate $(P_2Se_6)^{4-}$ unit. The indium compound contains the $(P_2Se_6)^{4-}$ lying perpendicular to the chain. The chromium and vanadium compounds contain the $(P_2Se_6)^{4-}$ lying along the chain similar to **II** but in a 4-fold coordinate fashion as opposed to the 6-fold coordinate binding in **II**. Thorium, due to its larger radius, is able to coordinate with a larger number of selenium atoms.

Electronic Spectroscopy. The electronic structures of the two compounds were analyzed using diffuse reflectance spectroscopy. The band-gap analysis of the compound indicates that $Cs_4Th_2P_6S_{18}$, **I**, has a band gap of 2.7 eV, Figure 10a, and $Rb_7Th_2P_6Se_{21}$, **II**, has a band gap of 2.0 eV,

(18) Cody, J. A.; Mansuetto, M. F.; Pell, M. A.; Chien, S.; Ibers, J. A. *J. Alloys Compd.* **1995**, *219*, 59−62. (b) Chondroudis, K.; Kanatzidis, M. G.; Sayettat, J.; Stephane, J.; Brec, R. *Inorg. Chem.* **1997**, *36*, 5859−5868. (c) Gauthier, G.; Jobic, S.; Brec, R.; Rouxel, J. *Inorg. Chem.* **1998**, *37*, 2332−2333. (d) Coste, S.; Kopnin, E.; Evain, M.; Jobic, S.; Brec, R.; Chondroudis, K.; Kanatzidis, M. G. *Solid State Sci.* **2002**, *4*, 709−716.
(19) Derstroff, V.; Tremel, W.; Regelsky, G.; Schmedt auf der Gunne, J.; Eckert, H. *Solid State Sci.* **2002**, *4*, 731−745.
(20) Chondroudis, K.; Kanatzidis, M. G. *J. Solid State Chem.* **1998**, *136*, 79−86.
(21) Tremel, W.; Kleinke, H.; Derstroff, V.; Reisner, C. *J. Alloys Compd.* **1995**, *219*, 73−82.

Table 6. Room-Temperature Raman Spectral Peaks (cm^{-1}) of $Cs_4Th_2P_6S_{18}$

$Cs_4Th_2(P_2S_6)_3$	$KlaP_2S_6$[15b]	$K_2FeP_2S_6$[21]	D_{3d} band assgnt
89 w	90		
97 w	111		
174 m			
188 m		183	ν_3 (A_{1g})
204 vw	204		
255 w		245	ν_{11} (E_u)
310 s			
358 w			
412 vs	387	391	ν_2 (A_{1g})

Table 7. Room-Temperature Raman Spectral Peaks (cm^{-1}) of $Rb_7Th_2P_6Se_{21}$

$Rb_7Th_2P_6Se_{21}$	$Mg_2P_2Se_6$[22]	D_{3d} band assgnt	$Pb_2P_2Se_6$[23]	C_{2h} band assgnt	$K_3La(PSe_4)_2$[17a]	T_d band assgnt
142 w					145	ν_2 (E_g)
150 m	149	ν_9 (E_g)	149	ν_4 (A_g)		
164 w	165	ν_8 (E_g)			163	ν_4 (F_2)
173 m						
185 vw						
221 vs	222	ν_2 (A_g)	215	ν_3 (A_g)		
233 s					237	ν_1 (A_1)
247 m			244	ν_{12} (B_g)		

Figure 10b. The band gaps correlate to the colorless and red colored crystals of compounds **I** and **II**, respectively. The band gaps are also consistent with other thio- and selenophosphate compounds studied.

Raman Spectroscopy. Raman spectra were collected on compounds **I** and **II**, Figure 11. The spectrum in Figure 11a shows the general features of the ethane-like $(P_2S_6)^{4-}$ unit of $Cs_4Th_2P_6S_{18}$, **I**. Spectral peaks and tentative band assignments are listed in Table 6. Three peaks are tentatively assigned to D_{3d} symmetry as compared to $K_2FeP_2S_6$.[22] The peaks at 188, 255, and 412 cm^{-1} are tentatively assigned to ν_3 (A_{1g}), ν_{11} (E_u), and ν_2 (A_{1g}), respectively. The spectrum for **I** also has peaks similar to those of $KLaP_2S_6$[15b] at 89, 97, and 204 cm^{-1} indicating the two compounds may have similar Raman active stretching modes. The unassigned peak at 310 cm^{-1} indicates one or more of the thiophosphate building blocks may have C_{2h} symmetry for the ν_{12} (B_g) stretching mode.

The spectrum of $Rb_7Th_2P_6Se_{21}$, **II**, shows the features of both the tetrahedral $(PSe_4)^{3-}$ unit and the ethane-like $(P_2Se_6)^{4-}$ unit, Figure 11b. Spectral peaks and tentative band assignments are listed in Table 7. Three peaks are assigned to T_d symmetry as compared to $K_3La(PSe_4)_2$.[17a] The peaks at 142, 164, and 233 cm^{-1} are tentatively assigned to ν_2 (E_g), ν_4 (F_2), and ν_1 (A_1), respectively. The $(P_2Se_6)^{4-}$ stretching is tentatively assigned to D_{3d} symmetry.[23] The three peaks at 150, 164, and 221 cm^{-1} are assigned to ν_9 (E_g), ν_8 (E_g), and ν_2 (A_g). The peak at 247 cm^{-1} indicates the $(P_2Se_6)^{4-}$ may also be assigned with C_{2h} symmetry with ν_{12} (B_g) stretching.[24] The final two unassigned peaks at 173 and 185 cm^{-1} are similar to unassigned peaks found in $Cs_4Th_2P_5Se_{17}$.[25]

Conclusions

We have prepared two novel thorium quaternary compounds with novel structures using the reactive flux method. $Cs_4Th_2P_6S_{18}$ formed a layered structure containing a tetramer of thorium polyhedra interconnected by the thiophosphate building blocks. $Rb_7Th_2P_6Se_{21}$ crystallized as a one-dimensional chain structure with two different selenophosphate building blocks interconnecting the thorium polyhedra. The two structures are related to known rare earth structures. Due to charge balance issues, alkali metals are inserted into rare earth sites to create the novel structures. As expected, by increasing the alkali metal to actinide metal ratio, the dimensionality of the structures reduce as compared to the rare earth structures. The band gap of the compounds correlates well with the observed crystal color. Raman spectroscopy confirmed the presence of the chalcophosphate building blocks. The alkali metal actinide chalcophosphate phase space continues to produce extremely diverse structures. Our continuing work explores the sodium actinide chalcophosphate phase space for novel structures and to study size effects of the alkali metals on the actinide chalcophosphate structures.

Acknowledgment. The authors thank Ms. Susie Miller for help with training on the X-ray diffractometer, Dr. Sandeep Kholi for training on the Raman and diffuse reflectance instruments, and Dr. Jennifer Burris and Dr. Dieter Hochheimer for collecting the single-crystal Raman spectrum on compound **I**. Funding for this work was provided by the Department of Energy, Heavy Element Chemistry grant ER15351.

Supporting Information Available: Additional crystallographic details and tables of atom positions, all bond distances and angles, and anisotropic thermal parameters. This information is available free of charge via the Internet at http://pubs.acs.org.

IC049101E

(22) Carrillo-Cabrera, W.; Sabannshausen, J.; von Schnering, H. G. *Z. Anorg. Allg. Chem.* **1994**, *620*, 489−494.

(23) Patzmann, U.; Brockner, W. *Z. Natursforsch.* **1987**, *42a*, 515.

(24) Becker, R.; Brockner, W. *Z. Natursforsch.* **1984**, *39a*, 357−361.

(25) Briggs Piccoli, P. M.; Abney, K. D.; Schoonover, J. R.; Dorhout, P. K. *Inorg. Chem.* **2000**, *39*, 2970−2976.